New Journal of Physics
The open-access journal for physics

Non-iterative coherent diffractive imaging using a phase-shifting reference frame

B Enders[1], K Giewekemeyer[1], T Kurz[2], S Podorov[3] and T Salditt[1,4]

[1] Institut für Röntgenphysik, Universität Göttingen, Friedrich-Hund-Platz 1, 37077 Göttingen, Germany
[2] III. Physikalisches Institut, Universität Göttingen, Friedrich-Hund-Platz 1, 37077 Göttingen, Germany
[3] School of Physics, Monash University, Victoria 3800, Australia
E-mail: tsaldit@gwdg.de

New Journal of Physics **11** (2009) 043021 (8pp)
Received 13 January 2009
Published 15 April 2009
Online at http://www.njp.org/
doi:10.1088/1367-2630/11/4/043021

Abstract. Lensless imaging is a high potential and currently intensely targeted research goal, in view of those fields of applications for which aberration-free high-resolution lenses are not available, for example for x-ray imaging. A recently proposed (direct inversion) variant of lensless imaging combines the advantages of two classical routes toward lensless imaging, the high-resolution characteristics of iterative object reconstruction, and the direct and deterministic nature of holographic reconstruction. Here, we use a simple standard optical setup using visible wavelength, a lithographic test object and a phase-shifting reference object to demonstrate the approach. Importantly, we show that a phase-shifting reference object, instead of the absorption mask proposed earlier, is sufficient for object reconstruction. This is relevant in view of the much easier implementation in future x-ray applications.

The scalar wavefunction obtained after transmission of a coherent incident wave through an unknown sample can be reconstructed from the modulus of its Fourier transform alone (reciprocal space), provided that additional constraints can be applied to the sample and/or the illumination function (real space) [1]–[3]. In other words, knowledge of the measurable far-field intensity pattern alone can be sufficient to reconstruct an unknown complex-valued object. Circumventing or at least alleviating the classical phase problem, this conclusion has fuelled intensive research in fields where high-resolution or aberration-free lenses are not available,

[4] Author to whom any correspondence should be addressed.

in particular in x-ray imaging [4]–[8]. It is obvious that a central issue of fundamental and practical importance in *coherent diffractive imaging* (CDI) relates to the nature of the additional constraints. A known modulus of the wavefunction in real space was the first constraint considered in this context [2], replaced later by the much less restrictive and experimentally more amenable constraint of a known support of the real-space wavefunction [1]. Building upon this seminal work, a family of related algorithms were developed to solve the nonlinear problem of object reconstruction by applying iterative constraint projections in real and reciprocal space [1, 9, 16–18]. In addition, more recent generalizations make it possible to reconstruct extended objects (no compact support) based on scanning the sample in an illumination function which is not translationally invariant [10, 19], and which itself can be reconstructed along with the sample [7, 17].

However, despite considerable progress in the iterative algorithms [9, 21], central issues of uniqueness, convergence, reconstruction speed, as well as optimum choice of initial phases and parameters in the algorithms, are yet unsolved in a strict mathematical sense. To overcome these limitations, and to achieve conceptual clarity in CDI, Podorov *et al* [11] have shown theoretically that a closed-form analytical solution exists, if the sample is placed in a uniformly illuminated rectangular hole. The sides of the rectangle must be at least two times larger than the extensions of the sample. Eight separate deterministic reconstructions of the object can then be obtained by application of a linear differential operator to the Fourier backtransform of measured far-field intensity. Since the rectangular frame acts as a reference r to the unknown object o, this scheme also falls into the category of holographic object reconstruction. Guizar-Sicairos and Fienup later generalized the approach to a greater class of extended reference structures [12]. The technique *holography with extended reference by autocorrelation linear differential operation* (HERALDO) [12] provides conceptual insight and a direct 'single shot phase-amplitude' retrieval for CDI problems. Compared with *in-line* or *off-axis* holography based on reference beams created by pinholes or waveguides [13, 14, 20], an extended reference r enables a reconstruction of the object o at a resolution not limited by the size of pinholes or apertures. Instead, HERALDO is only limited by inherent resolution of the far-field data, as it is generally the case for CDI, provided that the edges of r are sufficiently sharp. The beam-size related resolution limit and the complications associated with non-deterministic iterative reconstructions can then both be overcome simultaneously. At the same time, the overall geometry of r can be designed to separate images and the corresponding conjugates, avoiding problems associated with twin images.

Turning towards experimental implementation, one realizes that for hard x-ray imaging, where lensless techniques are most urgently needed to overcome the lack of high-resolution lenses, an appropriately sized opaque rectangular hole is extremely hard to achieve. In order to block a multi-keV beam, the necessary thickness of an absorbing mask counteracts a precise control of the edges as well as the positioning in or close to the sample plane. Contrarily, if a thin phase-shifting reference structure r is sufficient for direct inversion, the structure could be typically orders of magnitude thinner and hence also much better defined by lithography techniques. The purpose of this paper is twofold: (i) we want to generalize HERALDO to phase-shifting reference structures r and (ii) to demonstrate deterministic and direct inversion experimentally using visible light and a pure phase-shifting reference object.

Let us briefly review the basic setup for diffractive imaging to fix the coordinate system and the notation, see also figure 1. A monochromatic plane wave ψ_i with wave vector $\vec{k}$ propagates along the z-axis and illuminates the sample. In projection approximation, the exit wave directly behind the sample is $\psi_e = \tau \cdot \psi_i$, with $\tau(x, y)$ denoting the complex transmission function

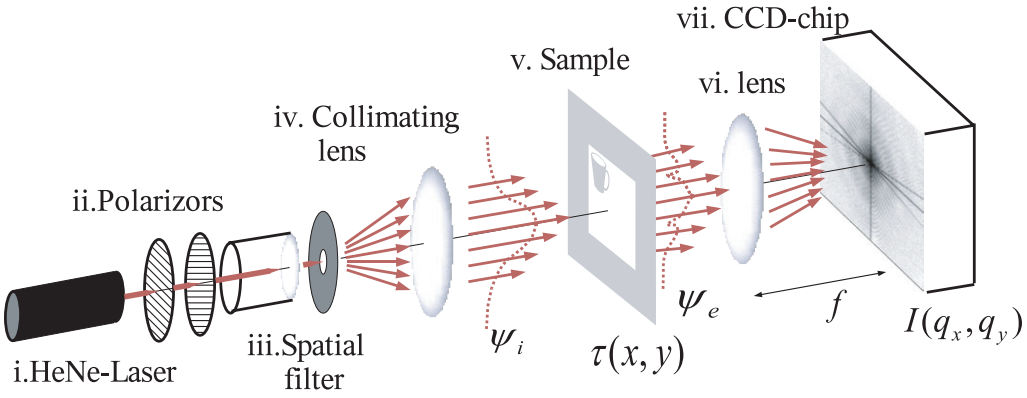

Figure 1. Schematic of a laser CDI experiment with the sample represented by a complex transmission function $\tau(x, y)$, followed by free space propagation of the exit wave ψ_e along the z-axis toward the detector plane, where the far-field intensity is recorded as a function of momentum transfer (q_x, q_y).

representing the projected index distribution of the sample. After a sufficiently long propagation distance along z into the Fraunhofer far-field regime, the measurable diffraction intensity $I(q_x, q_y)$ as a function of momentum transfer is written in kinematic (first Born) approximation as the squared modulus of the Fourier transform of the exit wave, $I(q_x, q_y) = |\mathcal{F}[\psi_e(x, y)]|^2$. The Patterson function $P(x, y)$ as the autocorrelation function in the sample plane is then obtained by the inverse Fourier transformation of $I(q_x, q_y)$,

$$P(x, y) = \mathcal{F}^{-1}[I(q_x, q_y)] \propto (\psi_e \otimes \psi_e)(x, y), \tag{1}$$

where the '$\otimes$' denotes the cross-correlation $f \otimes g(x, y) \equiv \int\int f(\nu, \mu) g^*(\nu - x, \mu - y) \mathrm{d}\nu \mathrm{d}\mu$. Let us assume that the exit wave behind the sample can be represented by a superposition of an object wave $o(x, y)$ and a reference wave $r(x, y)$, so that $\psi_e = r + o$. Following a calculation described in [12], it is further assumed that for a specific choice of r, there exists a 2D linear differential operator of order $n \in \mathbb{N}$, $\mathcal{L}^{(n)}$, with the following property:

$$\mathcal{L}^{(n)} r(x, y) = \sum_j C_j \delta(x - x_j)\, \delta(y - y_j) + h(x, y), \tag{2}$$

where δ denotes a Dirac delta function, $h(x, y)$ denotes a compact-supported function accounting for imperfections in the reference, i.e. the reference r is perfect for $\mathcal{L}^{(n)}$ if $h(x, y) = 0$. C_j are complex-valued arbitrary constants. Applying this operator now to $P(x, y)$ yields $\mathcal{L}^{(n)} P \propto \mathcal{L}^{(n)}[\psi_e \otimes \psi_e] = \mathcal{L}^{(n)}[r \otimes r + r \otimes o + o \otimes r + o \otimes o] = \mathcal{L}^{(n)} r \otimes r + \mathcal{L}^{(n)} r \otimes o + (-1)^n o \otimes \mathcal{L}^{(n)} r + \mathcal{L}^{(n)} o \otimes o$, to which equation (2) can be applied. Considering the shifting properties of the Dirac delta function in an autocorrelation, this will result in shifted copies of the object and the corresponding complex conjugated mirror images, for each delta function created by the operator:

$$\mathcal{L}^{(n)} P \propto \sum_j C_j r^*(x_j - x, y_j - y) \tag{3}$$

$$+ \sum_j C_j o^*(x_j - x, y_j - y) \tag{4}$$

$$+ (-1)^n \sum_j C_j^* o(x_j + x, y_j + y) \tag{5}$$

$$+ \mathcal{L}^{(n)} o \otimes o + h \otimes r + h \otimes o + (-1)^n o \otimes h. \tag{6}$$

Hence, reconstructions of the reference (3) and the object (4), (5) are obtained, whose origins are shifted to the positions $\vec{x}_j = (x_j, y_j)$ of the Dirac delta functions. As in off-axis holography, a single-step reconstruction without superposition of twin images can thus be obtained.

As a special choice of r, we consider now a centered rectangle with edge lengths $2a$ and $2b$ and arbitrary complex-valued transparencies τ_1 and τ_2 outside and inside the rectangle, respectively.

$$r(x, y) = \tau_1 + (\tau_2 - \tau_1)s(x, y), \tag{7}$$

which is a more generalized form of the *opaque/non-opaque* rectangular reference structure s, originally proposed in [11],

$$s(x, y) = \sum_j c_j \Theta(x - x_j)\, \Theta(y - y_j)\ , \tag{8}$$

where Θ is the Heaviside step function. The parameters are $c_j = [1, -1, 1, -1]$, $x_j = [-a, a, a, -a]$ and $y_j = [-b, -b, b, b]$. With the second-order differential operator $\mathcal{L}^{(2)} = \partial^2/(\partial x \partial y) = \partial_x \partial_y$, r obviously fulfills equation (2) with $C_j = c_j(\tau_2 - \tau_1)$.

Considering term (3), we obtain

$$\mathcal{L}^{(2)} r \otimes r = \sum_j c_j(\tau_2 - \tau_1) r^*(x_j - x, y_j - y) \tag{9}$$

$$= |\tau_2 - \tau_1|^2 \sum_j c_j s(x - x_j, y - y_j), \tag{10}$$

where the special properties of a centered rectangular reference, $\sum_j c_j = 0$ and $s^*(-x, -y) = s(x, y)$, have been applied to equation (9). The rectangle s is reconstructed with centers at the former edge positions (x_j, y_j) with prefactors c_j (see figure 2(b)). Compared with the previously considered *opaque/non-opaque* r, the magnitude however, is now modified by $|\tau_2 - \tau_1|^2$. There is no intensity outside the reconstructed s, although phase structures transmit throughout the entire sample. Furthermore, the absolute phase of the reference is not obtained in the reconstruction.

Let us now include the object with the transmittance $\tau_o(x, y)$. For separation purposes, we restrict the object position to the top left corner of the rectangle, i.e. in the area $[-a, 0] \times [0, b]$, such that

$$o(x, y) = \begin{cases} \tau_o(x, y) - \tau_2, & \text{for } (x, y) \in [-a, 0] \times [0, b], \\ 0, & \text{otherwise.} \end{cases} \tag{11}$$

According to terms (4) and (5) (i.e. $\mathcal{L}^{(2)} r \otimes o$ and $o \otimes \mathcal{L}^{(2)} r$), the conjugated and inverted reconstructions are in the bottom right corners of the reconstructed rectangles, whereas the unmirrored but shifted reconstructions are still in the top left corner (figures 2(c) and (d)). Within the stated assumptions, a straightforward calculation gives the reconstruction using equations (3)–(6), (10) and (11). For the first quadrant $(x, y > 0)$, one gets

$$\mathcal{L}^{(2)} P \propto \begin{cases} (\tau_o^{I-} - \tau_1)^*(\tau_2 - \tau_1), & (x, y) \in [a, 2a] \times [0, b], \\ (\tau_o^{I+} - \tau_1)(\tau_2 - \tau_1)^*, & (x, y) \in [0, a] \times [b, 2b], \\ |\tau_2 - \tau_1|^2, & (x, y) \in [a, 2a] \times [b, 2b], \\ 0, & (x > 2a \vee y > 2b). \end{cases}$$

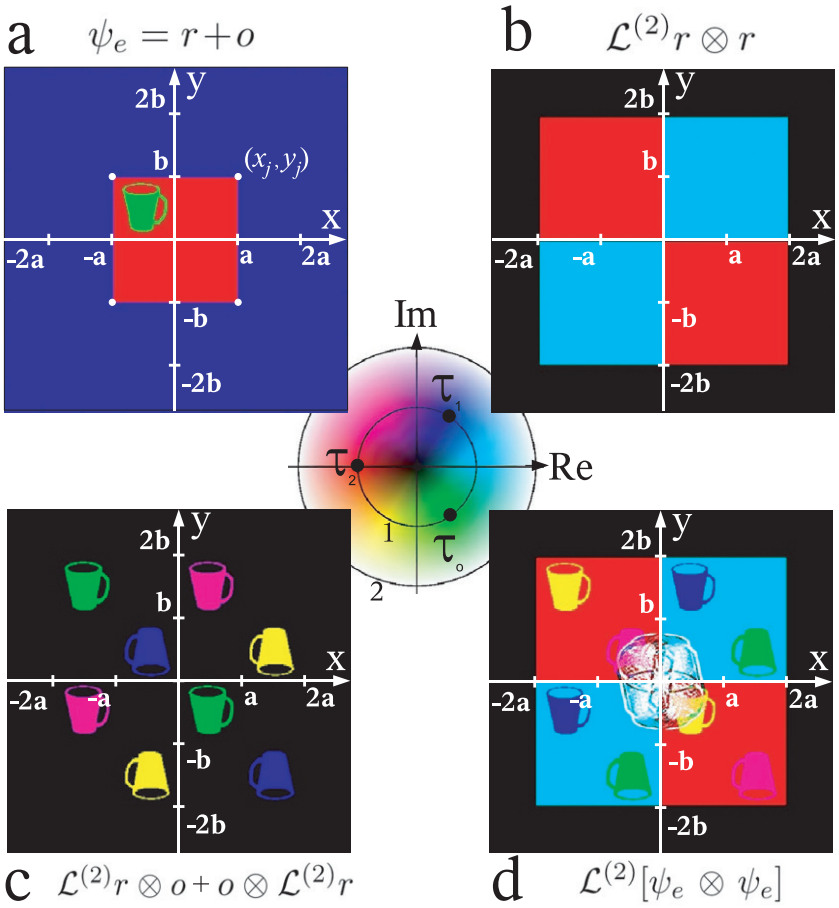

Figure 2. Numerical example of HERALDO with arbitrary transmissions τ_1, τ_2, and τ_o and rectangular reference. The phase is color-encoded according to its angle in the complex area (see center graph). The reconstructions (b–d) have been scaled by $|\tau_2 - \tau_1|^2$. (a) Scalar wave-function after transmission ψ_e with coordinates of the reference corners. (b) Reconstruction of the reference and (c) the 8 object reconstructions. (d) Superposition of all contributions including $\mathcal{L}^{(2)} o \otimes o$ located at the center.

with $\tau_o^{I+}(x, y) = \tau_o(x - a, y - b)$ and $\tau_o^{I-}(x, y) = \tau_o(a - x, b - y)$. As expected, a pure phase shift of $\mathbb{Z} \cdot 2\pi$ introduced by the reference will not result in any reconstruction. The object transmittance $\tau_o(x, y)$ is measured relative to the reference transmittance τ_1 and amplified by the difference $(\tau_2 - \tau_1)$. Thus, the highest possible signal amplification is given by a phase shift of π yielding $|\tau_2 - \tau_1| = 2$, a factor of two higher compared with the opaque reference frame. For the special case $\tau_o(x, y) = \tau_1$, the reconstructions of the reference and the object have two real values, as the object reconstruction values become zero just like outside the reconstructed rectangles (see figure 3(f)). In order to obtain the object transmittance values τ_o, knowledge of τ_2 and τ_1 is required. The relative contrast α of the object and the reference in the reconstruction is given by $\alpha = 1 - (\tau_2 - \tau_0)(\tau_2 - \tau_1)$.

The experimental setup consisted of a 10 mW HeNe laser (i) at $\lambda = 632.8$ nm, (ii) two linear polarizers for beam attenuation, (iii) a spatial filter consisting of a microscope objective

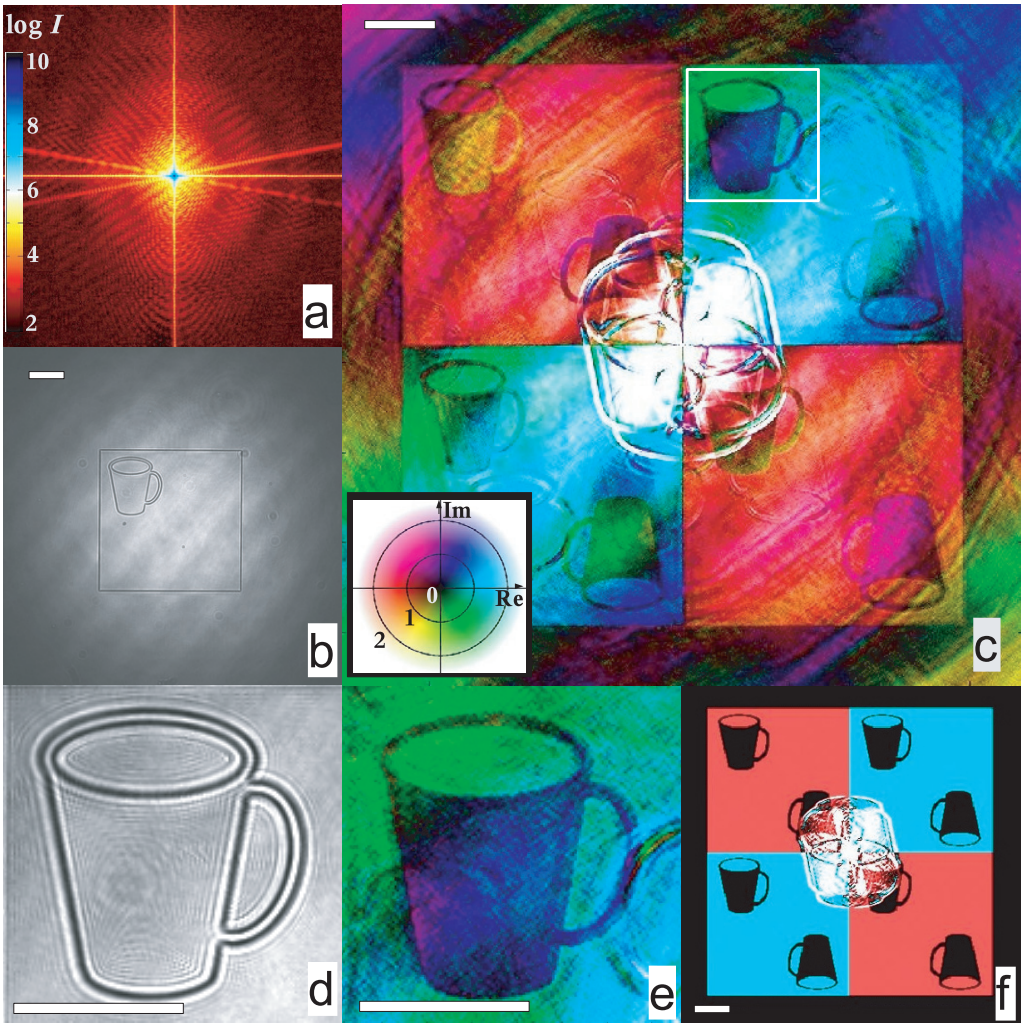

Figure 3. Experimental results. The length of the white scale bars corresponds to a length of 500 μm. (a) Diffraction image combined from 7 image series at different sensitivities; displayed is the logarithmic intensity $\log_{10} I$. (b) Inline microscope image that has been obtained using an additional 50 mm lens. (c) Reconstruction $\mathcal{L}^{(2)} P(x, y) = \mathcal{L}^{(2)} \mathcal{F}^{-1}[I(q_x, q_y)] \propto \mathcal{L}^{(2)}(\psi_e \otimes \psi_e)(x, y)$ normalized to the mean value. The phase is color-coded according to its angle in the complex area (see graph in bottom left corner). (d) Magnification of the object part in the microscope image. (e) Magnification of one of the 8 reconstructions (marked with a white square in (c)). (f) Numerical simulation of π phase shifting binary sample with uniform illumination.

(20×) and a 20 μm pinhole, followed by (iv) a collimating lens to obtain a quasi-plane wave illumination with a Gaussian intensity profile of variance $\sigma_{ill} \simeq 1.26$ mm. The sample (v) is mounted on an *xyz*-stage and consisted either of a document type slide or a patterned layer of photoresist deposited on an optical plane glass substrate (see below). Behind the sample a lens (vi) with 50 mm focal length was placed to image the diffraction pattern formed in the rear focal plane onto the CCD sensor (vii). The images were collected by a CoolSnap EZ Progressive Scan

CCD camera (Photometrics, USA), operating with a Sony ICX285 CCD-chip with 1392×1040 pixels at 6.45 μm pixel size. To increase the dynamic range in the image, a set of image series at different sensitivities, i.e. different exposure times, were stitched to a final image of high dynamic range. The exposure time between different elements of the set was increased by a factor of 10. Overexposed pixels were discarded. Altogether, the set comprised seven series, with exposure times from 10^{-6} to 1 s, each series consisting of 100 individual background corrected images. The combined final image was 761×761 pixels in size and had a maximum value of about 10^{10} registered counts in the highest intensity pixels, compared with a noise level of over 10^2 per pixel, resulting in a dynamic range of roughly 10^8, see figure 3(a). The image analysis software was written in MATLAB.

The sample consisted of a patterned layer of positive photoresist (AR-P3120, Allresist, Germany), spin-coated onto an optically plane glass substrate, and developed using contact lithography (Mask Aligner MJB4, Suess Microtech, Germany) from a chromium mask (ML&C Jena, Germany). Figure 3(b) shows the pattern of a coffee mug positioned into a square aperture of 2 mm length. After developing, the remaining resist (coffee mug, reference structure outside the rectangle) had a thickness of about 550($\pm$10) nm, yielding a phase shift of $\simeq 1, 13\pi$ with an optical index of $n = 1.65$.

The experimental setup is depicted in figure 1. Figure 3 comprises the results. Figure 3(b) shows an in-line transmission image of the sample. It was obtained by placing two lenses of $f = 50$ mm behind the sample. The absorption contrast of the sample is negligible and edge contrast appears, if an according shift from the focal plane (defocus) is intentionally set, as is well known for near field (Fresnel) imaging. Figure 3(c) shows the eight copies of reconstructions, which are all visible in either intensity or phase contrast. Figure 3(f) shows the corresponding numerical simulation for uniform illumination and perfect reference. The reconstructions obtained from the experimental data deviate from the simulation, most likely due to the non-uniform illumination and the non-perfect combination of different exposures. The noise in the reconstruction is due to Poissonian noise in the diffraction images and to random phase perturbations, e.g. as introduced by surface roughness. In particular, the Fourier inversion process requires diffraction patterns of large dynamical range, which are difficult to obtain with current CCD detectors. The aquisition of multiple frames as used here is a compromise, since it is inefficient and also induces noise.

However, according to our experience, the illumination conditions are the most critical point for reconstruction. This issue is understandably more difficult for the phase shifting r than for opaque r, where the absorbing frame blocks the tails of the beam. Note that for phase objects it is important to determine the center of the diffraction pattern very accurately, before performing the Fourier transform. Otherwise, plane wave-like phase modulations occur. Given imperfections in r, the (last) three terms in (6) may not vanish. While this goes beyond the scope of this work, we note that if $h(x, y)$ is a spread out function, i.e. due to phase perturbations from air, substrate related phase shifts etc, (6) will yield a noisy background signal. In the opposite case of localized imperfections, sudden changes in the phase shift are amplified by differentiation, and therefore make the imperfections 'detectable by $\mathcal{L}^{(n)}$'. Hence, in this case (6) is expected to yield disturbing background patterns, which are much harder to distinguish in the reconstruction. Such effects can be caused by artifacts in the pattern definition of r, dust, layer thickness variation, deformed edges, as well as from non-uniform and unknown illumination. However, the two terms containing h can be evaluated to predict and to model imperfections, opening up a route for future correction strategies. In summary, we have demonstrated that

direct-inversion CDI introduced in [11] and generalized in [12] is experimentally feasible for optical wavelengths. Importantly, it can be generalized to phase shifting reference structures and/or samples. This generalization is of great importance for the next step to use the approach in hard x-ray imaging, where extended phase contrast objects can be prepared more easily than absorption masks or reference beam pinholes. Moreover, it is likely that the reference mask and the sample do not need to be positioned exactly in the same plane, if a correction for Fresnel propagation between the reference object and the sample is taken into account, somewhat similar to a phase-shifting mask [15]. In contrast to all previous variants of CDI, the reconstruction would still be based on a fast and deterministic reconstruction step. The fact that the object should be smaller than the reference frame could be held against this approach, since many of the most interesting samples in materials and life science applications are extended. However, the eight different copies of the object appear as linear superpositions. It remains to be verified whether, by scanning an extended sample through the reference frame, the different superpositions could be decomposed in a deterministic manner, if three quarters of the rectangle have been reconstructed by an earlier step.

Acknowledgments

We acknowledge financial support by Deutsche Forschungsgemeinschaft through *SFB*755 *Nanoscale Photonic Imaging*.

References

[1] Fienup J R 1982 *Appl. Opt.* **21** 2758
[2] Gerchberg R W and Saxton W O 1972 *Optik* **35** 237
[3] Paganin D M 2006 *Coherent X-Ray Optics* (Oxford: Oxford University Press)
[4] Miao J *et al* 1999 *Nature* **400** 342
[5] Miao J *et al* 2002 *Phys. Rev. Lett.* **89** 088303
[6] Chapman H N *et al* 2006 *Nat. Phys.* **2** 839
[7] Thibault P *et al* 2008 *Science* **321** 379
[8] Schroer C G *et al* 2008 *Phys. Rev. Lett.* **101** 090801
[9] Marchesini S 2007 *Rev. Sci. Instrum.* **78** 011301
[10] Rodenburg J *et al* 2007 *Phys. Rev. Lett.* **98** 034801
[11] Podorov S G, Pavlov K M and Paganin D M 2007 *Opt. Express* **15** 9954
[12] Guizar-Sicairos M and Fienup J R 2007 *Opt. Express* **15** 17592
[13] Eisebitt S *et al* 2002 *Nature* **432** 885
[14] Fuhse C, Ollinger C and Salditt T 2006 *Phys. Rev. Lett.* **97** 254801
[15] Johnson I *et al* 2008 *Phys. Rev. Lett.* **100** 155503
[16] Song C *et al* 2008 *Phys. Rev. Lett.* **100** 025504
[17] Quiney H M *et al* 2006 *Nat. Phys.* **2** 101
[18] Eisebitt S *et al* 2004 *Appl. Phys. Lett.* **84** 3373
[19] Abbey B *et al* 2008 *Nat. Phys.* **4** 394
[20] Stadler L-M *et al* 2008 *Phys. Rev. Lett.* **100** 245503
[21] Barakat R and Newsam G 1984 *J. Math. Phys.* **25** 3190